Chemical Engineering & Processing: Process Intensification 179 (2022) 109065

Contents lists available at ScienceDirect

Chemical Engineering and Processing - Process Intensification

journal homepage: www.elsevier.com/locate/cep

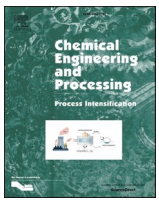

Response surface methodology for continuous biodiesel production from Jatropha curcas oil using Li/pumice as catalyst in a packed-bed reactor assisted with diethyl ether as cosolvent

L. Díaz *, D. Escalante, K.E. Rodríguez, Y. Kuzmina, L.A. González

Chemical Engineering Department, University of La Laguna, Avda. Astrofísico Fco. Sánchez s/n, La Laguna, Tenerife, Canary Island 38200, Spain

ARTICLE INFO

Keywords:
Biodiesel
Heterogeneous catalyst
Packed bed
Continuous production
Cosolvent
Response surface methodology

ABSTRACT

A packed-bed catalytic configuration reactor using pumice granules loaded with lithium (Li/Pumice) as a heterogeneous catalyst was developed for biodiesel production in continuous. For this purpose, *Jatropha curcas* oil was used as an alternative feedstock to edible oils and diethyl ether was used as a cosolvent to eliminate the limitations of mass transfer between the phases. In this work, the response surface methodology was applied to optimize the fatty acid methyl esters (FAME) yield in biodiesel production. The flow rate (0.7–1.4 mL min^{-1}), the methanol/oil molar ratio (6:1–20:1) and the cosolvent/methanol molar ratio (0.5:1–1.5:1) were the independent variables studied. The effects of these factors over the FAME yield using Li/Pumice as catalyst were evaluated according to a Box-Behnken design. The optimum conditions for the maximum FAME yield (100%) were 1.4 mL min^{-1}, 20.0 methanol/oil molar ratio and 0.57:1 cosolvent/methanol molar ratio.

1. Introduction

Biodiesel is a fuel from renewable biological sources such as vegetable oils and animal fats. The production of biodiesel involves chemical reactions between the free fatty acids (FFA) and the triglycerides present in the oils or fats and an alcohol (methanol, ethanol, etc.) to generate a fatty acid methyl ester (FAME) and glycerol mixture product. Three types of synthesis processes have been used for biodiesel production: transesterification by basic catalysis, transesterification by acid catalysis (with simultaneous esterification of FFA) and non-catalytic supercritical alcohol transesterification [1–4]. Current trends focus on the study of the transesterification reaction using heterogeneous catalysts and non-edible raw materials, such as oils from energy crops or waste cooking oils [5–7].

Biodiesel synthesis can be carried out by continuous or discontinuous operation mode [8]. Currently, on the industrial scale biodiesel production, slurry batch reactors are usually used to carry out the transesterification reaction due to homogeneous catalysts are employed. Batch processes are characterized by low productiveness and high operating costs. However, the productivity of a process can be greatly increased with the implementation of continuous operations; in this case, the use of packed-bed catalytic reactor may allow the design of a continuous and efficient biodiesel production process that will improve its economy [9], due to the easy separation of the reaction products since the catalyst is confined to the bed, the possibility of reusing the catalyst or the removal of the necessary biodiesel washing step when a homogeneous catalyst is used, as well as the consequent management and treatment of the wastewater generated in this process [10]. However, alcohol and triglycerides are not soluble, causing the reaction to occur in the alcohol-triglycerides interface. A solution to improve the mutual solubility of methanol and triglycerides and decrease the mass transfer resistance during the chemical reaction is using a cosolvent [11–14].

The use of cosolvents to improve the transesterification process in the production of biodiesel is a subject that is increasing the interest of researchers [15]. Cosolvents, such as tetrahydrofuran (THF), diethyl ether (DEE), 1,4-dioxane, etc., have polar and non-polar sites, which causes a decrease in surface tension between the alcohol and triglyceride phases and creates a homogeneous reaction system, so the reaction can occur in a mild condition with less reaction temperature and less reaction time [16,17], and with an increased FAME yield [18,19]. Soriano and Venditti [20] studied the transesterification reaction of canola seed oil using THF as cosolvent and evaluated the progress of the reaction by ^{1}H NMR. The authors observed an increase in biodiesel yield due to

* Corresponding author.
E-mail address: laudiaz@ull.es (L. Díaz).

https://doi.org/10.1016/j.cep.2022.109065
Received 19 May 2022; Received in revised form 5 July 2022; Accepted 19 July 2022
Available online 21 July 2022

significant reduction in mass transfer resistance between phases of oil and methanol. Mohammed-Dabo et al. [21] also investigated the transesterification reaction of *Jatropha curcas* seed oil for the biodiesel production using THF as cosolvent and the THF/methanol ratio was optimized. The authors also confirmed an increase in biodiesel yield with an optimum THF/methanol ratio of 1:1% (v/v). The authors conclude that transesterification using cosolvents is a way to reduce energy cost, since the stirring requirements would be lower, as well as the reaction time. Hashemzadeh and Sadrameli [22] investigated the continuous biodiesel production using a packed bed reactor with a solid based catalyst, linseed oil and DEE as cosolvent. The authors conclude that DEE cosolvent reduces mass transfer limitations, leading to high yields of FAME. The addition of DEE to the reaction system increased the FAME yield from 75.83% to 98.08% under the following conditions: DEE/methanol molar ratio of 1.19:1, methanol/oil molar ratio of 9.48:1 and a flow rate of 1.37 mL/min. On the other hand, Encinar et al. [12] report that the use several cosolvents as DEE, THF, acetone, dibutyl ether (diBE), tert-butyl methyl ether (tBME) and diisopropyl ether (diIPE) produce a significant improvement in the transesterification reaction due to biodiesel with high methyl ester content was produced. The maximum methyl ester contents (97–98%) were achieved when DEE, tBME and THF were used under the following conditions: cosolvent/methanol molar ratio of 1:1, methanol/oil molar ratio of 9:1, 0.7 wt% KOH, 700 rpm and 30 °C.

In this work, a study on continuons biodiesel production using a solid catalyst in a packed-bed reactor assited with diethyl ether as cosolvent was carried out using Box–Behnken response surface methodology (RSM) for maximizing the FAME yield. For this purpose, a catalytic packed-bed reactor with inner diameter of 1 cm and height of 20 cm and pumice granules loaded with lithium (Li/Pumice) as catalyst was employed. BBD (3 factors and 3 levels) was employed to investigate the effect of the flow rate (0.7–1.4 mL/min), the methanol/oil molar ratio (6:1–20:1) and the cosolvent/methanol molar ratio (0.5:1–1.5:1) on the FAME yield at a constant reaction temperature of 40 ºC. Box-Behnken design (BBD) was selected because requires fewer experiments than other RSM designs with the same number of factors and for being more efficient than other designs [23–25]. Although Artificial Intelligence (AI) is one of the fastest growing technologies today, it has some limitations such as data availability, cost and implementation time; for this reason, RSM has been selected for this study. RSM operates with a small number of experimental runs, while AI methods need more data. RSM has proven to be an effective method to combine the optimization of several independent variables and their responses [26].

2. Experimental

2.1. Materials

Jatropha curcas oil was used as feedstock for the biodiesel production because it does not compete with human food due to the existence of certain harmful components. In addition, it presents several ecological, energetic and economic advantages related to its commercial use [27]. *Jatropha curcas* oil was extracted from its seeds with n-hexane as solvent using a soxhlet extractor. The oil obtained was esterified to reduce the free fatty acids content. Both processes are described in a previous work [28]. The physical properties of *Jatropha curcas* oil are: $\nu_{40^{\circ}C}$=17.5 cSt, $\rho_{15^{\circ}C}$=931.4 kg m^{-3} and acid value=0.1 mg KOH g^{-1}. Methanol (99.8% purity) and diethyl ether (99.7% purity) were supplied by Sigma-Aldrich (Germany). Lithium nitrate anhydrous (≥ 98%) was acquired from Fisher Scientific (Belgium) and pumice particles were purchased from Panreac (Spain). Methyl heptadecanoate (99.9% purity), supplied by Fluka Analytical (Germany), was used as internal standard for gas chromatography.

2.2. Catalyst preparation

Li/Pumice (5 wt% of Li) was employed as solid catalyst for the transesterification reaction. Pumice particles of 1.4–3.0 mm were submitted to impregnation with lithium nitrate anhydrous ($LiNO_3$). Lithium impregnated pumice catalyst was prepared by a wet impregnation method. First, Li precursor was fully dissolved in deionized water, and the precursor solution was added to 10 g of pumice support previously weighed. Then, the impregnated pumice particles were dried overnight at 100 ºC and finally calcined at 650 ºC for 5 h under air flow in a muffle furnace.

2.3. Catalyst characterization

The surface morphology of pumice and lithium supported pumice (Li/Pumice) was monitored using a scanning electron microscope (SEM) (Jeol LTD, mod. JSM-6300, Tokio, Japan). Due to the non-conductive nature of the pumitic materials, all samples were coated with a thin layer of sputtered silver.

BET surface area and physical properties of the pumitic materials were determined by nitrogen adsorption–desorption isotherms recorded on a surface pore size analyzer (Gemini V, Micromeritics) and a mercury porosimetry (Autopore IV mercury porosimeter, Micromeritics). From these results, the pore size distributions of the materials were obtained.

X-ray diffraction patterns (XRD) of the materials were performed with a PANalytical X'Pert diffractometer, equipped with a primary monochromator and X'Celerator detector, using Cu $K\alpha_{1,2}$ radiation (45 kV and 40 mA) as the X-ray source. The patterns were recorded in 4–80º 2θ range.

Pumice and Li/Pumice materials were examined by Fourier transform infrared spectrometry (FTIR). FTIR spectra were measured within the 4000 to 400 cm^{-1} wavenumber regions, with a resolution of 2 cm^{-1}, using an Agilent Cary 630 spectrometer coupled with the attenuated total reflectance (ATR) module (ZnSe). ATR unit was controlled by the MicroLab software and the program Resolutions Pro-was used for data processing.

2.4. Continuous transesterification in packed-bed reactor

The continuous biodiesel production was carried out in a packed-bed catalytic reactor configuration with Li/Pumice as heterogeneous catalyst. The schematic diagram of the packed-bed catalytic reactor is illustrated in Fig. 1. First, the catalytic reactor (jacketed glass reactor) was loaded and packed with 10 g of Li/Pumice. Secondly, *Jatropha curcas* oil was placed in a 1000 mL heated tank, equipped with a reflux condenser and a mechanical stirrer. When the selected reaction temperature (40 ºC) was reached, methanol (MeOH) and DEE (pre-mixed in desired amounts) was added to the tank with continuous stirring (400 rpm). The mixture was heated up to the reaction temperature and then fed into the packed-bed catalytic reactor using a peristaltic pump at a constant flow rate (0.7–1.4 mL/min). The feed solution was supplied to the bottom of the cylindrical reactor (20 cm length and 1 cm inner diameter) packed with Li/Pumice catalyst particles. The reaction products were collected at the outlet of the reactor for 90 min and evaporated for removing excess methanol and DEE. Then, the liquid product was settled in a funnel by separating the biodiesel from glycerol. The biodiesel product obtained (upper phase) was analyzed by gas chromatography (GC) to estimate the FAME content in biodiesel product obtained in each run.

The bed porosity (ε_b=0.71) was deteminated using the Eq. (1) [29, 30].

$$\varepsilon_b = 1 - \frac{W_c/\rho_c}{\pi h(d/2)^2} \quad (1)$$

Where W_c is the weight of the solid catalyst, ρ_c is the density of the solid

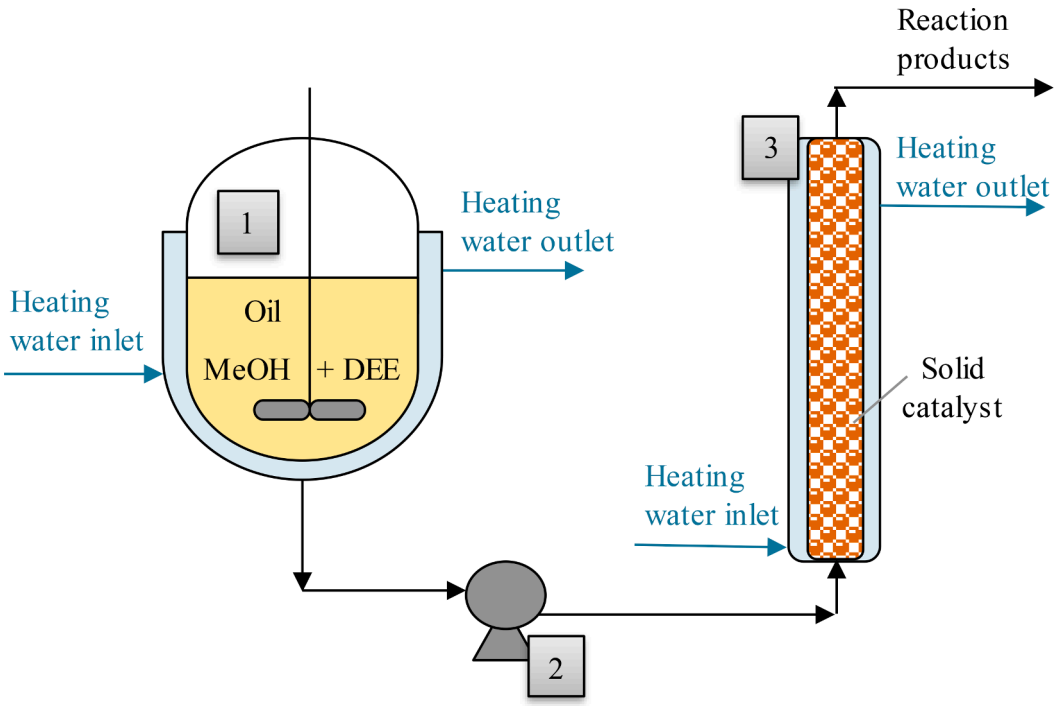

Fig. 1. Reaction system for continuous biodiesel production: 1) mixing tank, 2) peristaltic pump, 3) packed-bed reactor.

catalyst and d is the inner diameter of the reactor.

2.5. Analytical methods

FAME content analyzes were performed in accordance with UNE-EN 14,103 [31], using a 3900 Varian gas chromatograph (GC-FID). Separations were accomplished using a 50 m long CP-SIL 88 capillary column (0.25 mm I.D. and 0.25 μm film thicknesses) at a constant hydrogen flow rate of 30 mL min^{-1}. The injector and FID detector temperatures were set a 250 °C. The oven was initiated at 160 °C for 5 min, then, it was elevated to 180 °C at 4 °C min^{-1} and held for 2 min, elevated to 225 °C at 15 °C min^{-1} and maintained for 5 min, finally elevated to 240 °C at 15 °C min^{-1} and held for 1 min. Helium was applied as a carrier gas (1.0 mL min^{-1}) and nitrogen as make-up gas (30 mL min^{-1}). Samples (0.5 μL) were injected with a split ratio of 20:1.

2.6. Response surface methodology

RSM based on three-level and three-factor BBD, was implemented to study the effects of the main independent factors and the interactive effects between the parameters on the dependent response variable. The three steps of the RSM were developed: a) design of experiments, b) response surface modeling and c) optimization. Specifically, the BBD was used to find the optimal conditions for maximizing the FAME content. The BBD based on RSM was selected in this work as this design is more effective than the other RSM designs such as full factorial designs or central composite design. BBD involves a smaller set of experimental data for the case of three independent variables [27,28].

In this work, the flow rate (X_1), the methanol/oil molar ratio (X_2) and the cosolvent/methanol molar ratio (X_3) are considered as independent variables that affect the transesterification reaction. Three different levels were applied for each variable: low (−1), medium (0), and high (+1). FAME content (Y) was selected as the dependent variable (response). Table 1 summarizes the independent and dependent variables used for the design of experiments, as well as the ranges and levels of the three independent reaction variables. The other operating parameters were as follow: amount of catalyst of 10 ± 0.01 g, reaction temperature of 40 ± 1.0 °C, agitation rate of 400 rpm and reaction time of 90 ± 0.017 min.

Table 1
Variables, levels and ranges of the transesterification reaction variables in BBD.

		Symbol	Level of factors		
			−1	0	1
Independent variables (factors)	Flow rate (mL min^{-1})	X_1	0.7	1.05	1.4
	MeOH/oil molar ratio	X_2	6	13	20
	DEE/MeOH molar ratio	X_3	0.5	1	1.5
Dependent variable	FAME (%)	Y	Optimize		

2.7. Statistical analysis

Results were statistically analyzed by using Statgraphics Centurion XVI, version 16.1.18 (StatPonit Technologies, Inc.). The relationship between the three independent variables (X_1, X_2 and X_3) and the response (FAME content) was expressed using a polynomial regression model as shown in Eq. (2).

$$Y = \beta_0 + \sum_{i=1}^{3} \beta_i X_i + \sum_{i=1}^{3} \beta_{ii} X_i^2 + \sum_{i=1}^{2} \sum_{j=i+1}^{3} \beta_{ij} X_i X_j \quad (2)$$

where Y is the response variable (% FAME), X_i and X_j are the different independent variables ($i \neq j$), β_0 is the intercept parameter, β_i are the linear coefficients, β_{ii} are the squared coefficients and β_{ij} are the interaction coefficients.

Analysis of variance (ANOVA) was applied to evaluate the significance and the fitness of the regression model as well as the effect of significant individual terms and their interaction on the response variable [32]. 3D response surface profiles and contour plots of the fitted polynomial regression equation were generated to display the relationships between the response and the independents variables.

3. Results and discussion

3.1. Catalyst characterization

The surface topography of pumice (Fig. 2a, b, and c) and pumice impregnated with lithium (Fig. 2d, e, and f) was analyzed using scanning electron microscopy (SEM). SEM images show the high porosity of both pumitic materials. The porous structure of support material varied after the impregnation process; when pumice was impregnated with the lithium precursor, the porosity of the raw material seems to decrease. The decrease in porosity is confirmed by the results obtained by mercury porosimetry shown in Table 2. Porosity decreased from 44.43% (pumice) to 37.10% (Li/pumice) after the impregnation process.

The main characteristics of the pumice and Li/Pumice are presented in Table 2. BET specific surface area (S_{BET}) and average micropore width (D) are shown for both materials. As can be seen there is a decrease of the S_{BET} and the average micropore width, when support material (pumice) is impregnated with lithium precursor due to pores blocking. The average pore diameter of the materials is between 2 and 50 nm, so it

Table 2
Textural properties of catalytic solid.

Material	N_2 adsorption		Mercury porosimetry			
	S_{BET}(m^2 g^{-1})	D (nm)	A(m^2 g^{-1})	ε(%)	D (V) (nm)	D (4 V/A) (nm)
Pumice	0.71	4.19	16.30	44.43	1534.1	91.9
Li/ Pumice	0.39	3.71	6.90	37.10	1782.4	118.3

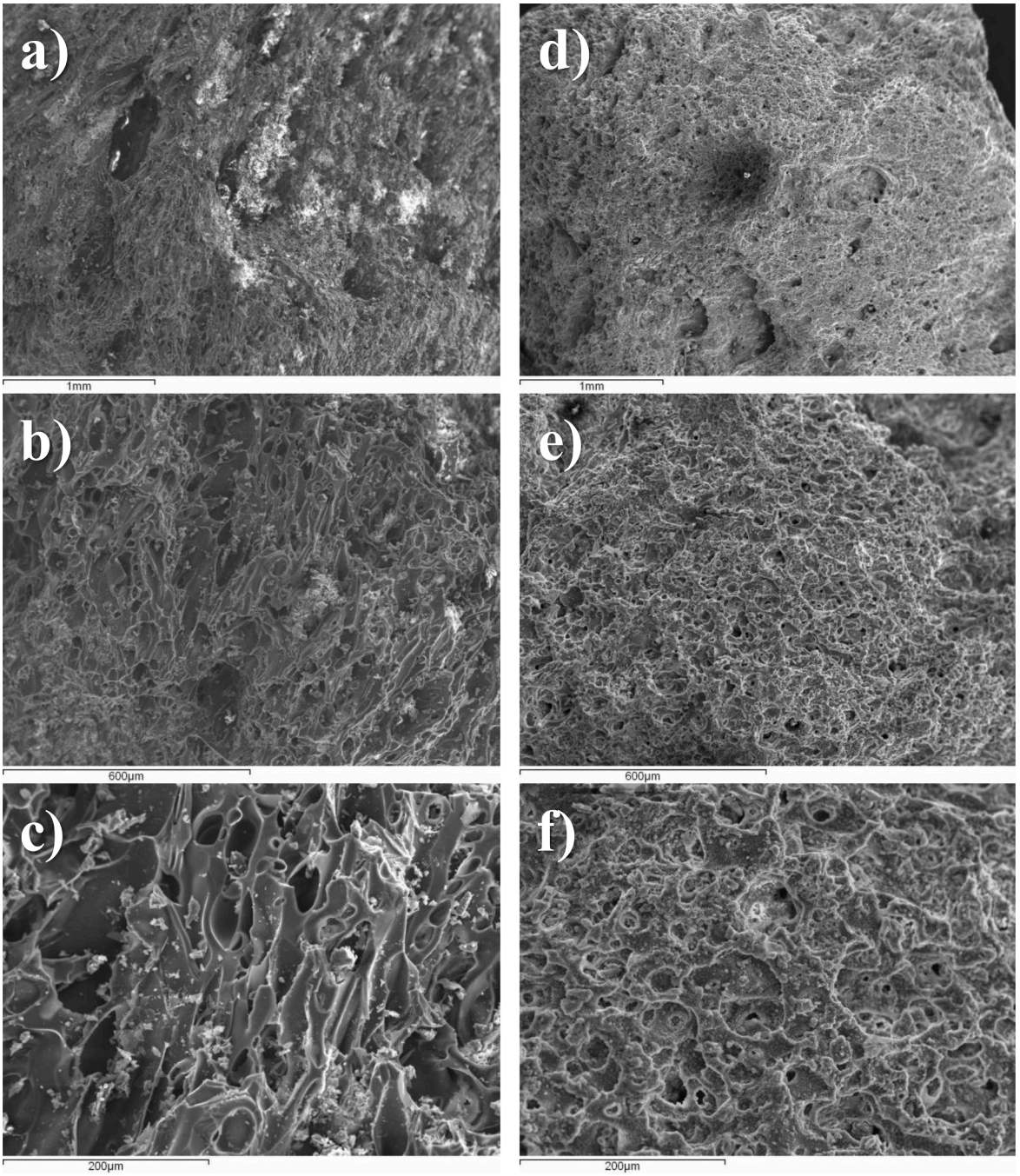

Fig. 2. SEM images for Pumice (a, b y c) and Li/Pumice (d, e y f).

can be considered that none of the materials are microporous. The physical properties of the pumitic materials obtained by mercury porosimetry are also shown in Table 2. The values of specific surface (A), porosity (ε) and average pore diameter (D) are shown. The specific area also decreased after the impregnation process and the average pore diameter, in the range of meso-macropores, increased.

In Fig. 3 pore size distributions from N_2 adsorption isotherms and mercury porosimetry are compared for the studied materials, showing an irregular pore structure of both materials, in the micro-mesopore range (Fig 3a) and in the meso-macropore range (Fig 3b). The greater intrusion volume of mercury versus nitrogen, indicates that the materials are mainly meso-macroporous; which is an advantage because the average pore diameter is greater than the diameter of the triglyceride molecule (5 nm), therefore, it is expected that the triglyceride molecules will diffuse easily through the pores of the catalyst and, consequently, there will be an efficient contact between the reactants and the active sites present on the surface of the catalyst, which are necessary for the reaction transesterification occurs [33].

Diffraction patterns of pumitic materials are shown in Fig. 4. Crystalline phases do not appear in the XRD pattern of pumice, a broad and diffuse peak is observed in the range of $2\theta = 20–30^{o}$, typical of amorphous aluminosilicates; specifically, it reflects the amorphous structure of silica (SiO_2), since it is the majority oxide present in pumitic materials [34–36]. However, after the impregnation process, XRD pattern of Li/Pumice presents crystalline phases, which can be attributed to the formation of the phases $LiAl(Si_2O_6)$, $Li(AlSi_4O_{10})$ and $LiAl(SiO_3)_2$

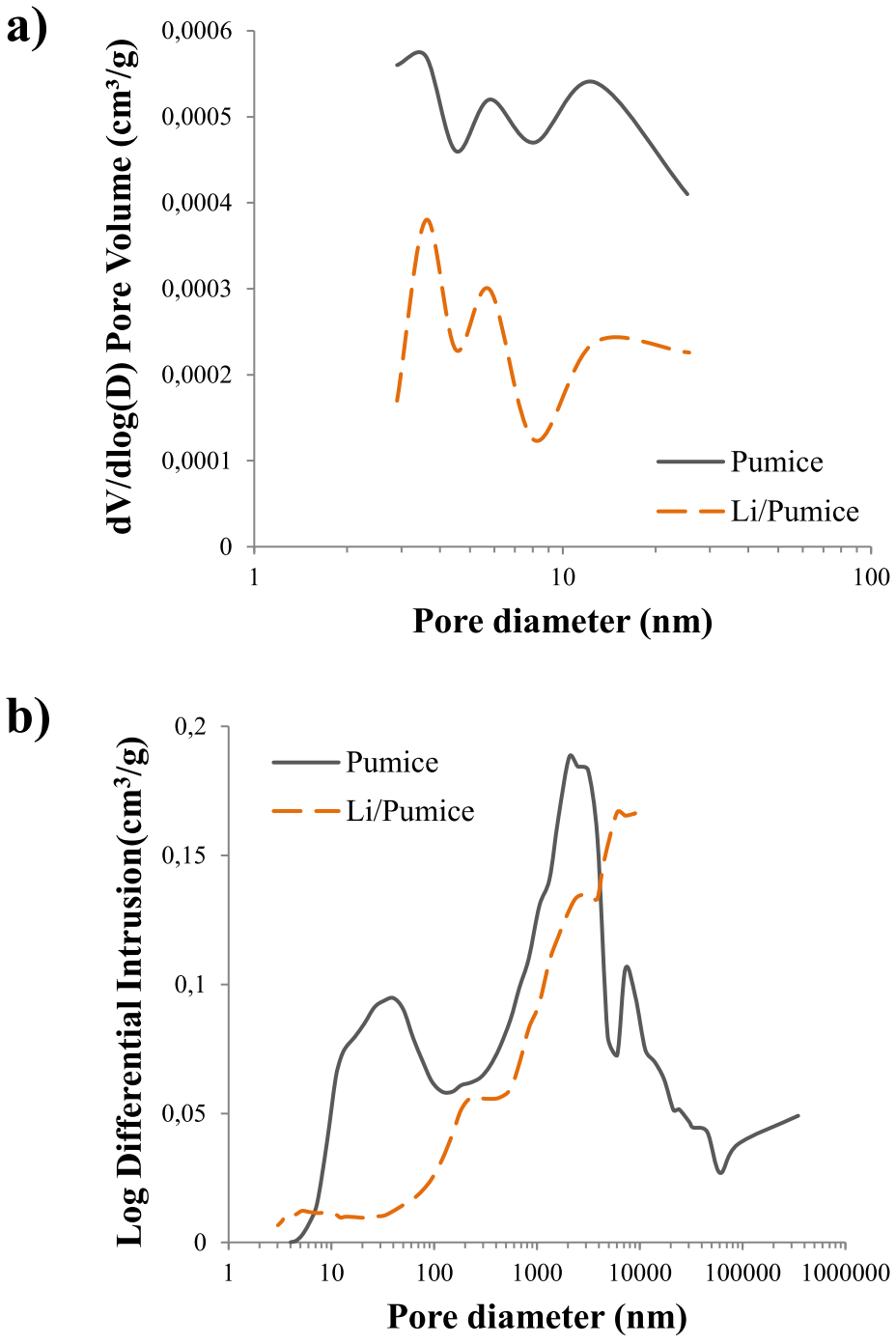

Fig. 3. Pore size distribution from (a) N_2 adsorption and (b) mercury porosimetry of the pumitic materials.

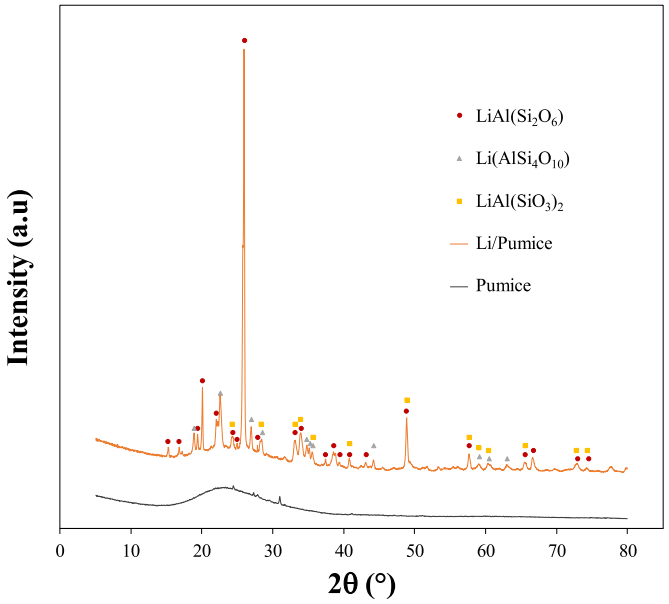

Fig. 4. XRD patterns of the Pumice and Li/Pumice.

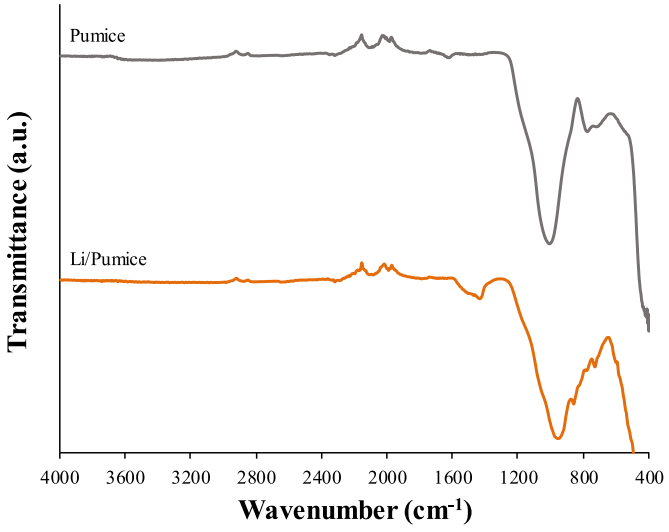

Fig. 5. FTIR spectra of the Pumice and Li/Pumice.

obtained through the QualX software, using the POW_COD_2007 database (Fig. 4).

From a comparison of the FTIR spectra of the pumitic materials, there is no significant difference in the interpretation and identification of the peaks; however, the most intense signal observed in the FTIR spectrum of pumice, located at 1009 cm^{-1}, undergoes a shift towards lower wavenumber values after impregnation of the material with the lithium precursor (976–994 cm^{-1}). The broad band located between 600 and 1200 cm^{-1} is characteristic of aluminosilicates and is attributed to the internal vibration of the TO_4 tetrahedrons (T = Al or Si). The wide range of this band is mainly attributed to the amorphous nature of the materials, as well as the short-range ordering of the Si and Al tetrahedrons [37].

3.2. Experimental design and statistical analysis

BBD with three levels and three factors was carried out to optimize the simultaneous effect of three independent variables (flow rate, MeOH/oil molar ratio and DEE/MeOH molar ratio) on the FAME content of biodiesel product from continuous transesterification process. According to the BBD, a total of 15 experiments (runs) were performed in randomized order with three replicates of the central point. The complete design matrix obtained from BBD design for experiment and predicted results are tabulated in Table 3. The uncertainty of each parameter is included in the table header.

The fit between the response variable and the independent variables corresponds to a second-order polynomial, as shown in Eq. (3).

$$Y = 26.30 - 6.17X_1 + 5.12X_2 + 32.83X_3 + 0.97X_1X_2 - -13.29X_1X_3 + 0.10X_2X_3 + 0.41{X_1}^2 - 0.13{X_2}^2 - 14.1{X_3}^2 \quad (3)$$

This equation allows to visualize the effects of each parameter and their interactions on the response, since a positive sign in front of the terms indicates a synergistic effect, while a negative sign indicates an antagonistic effect [38].

The quality of the model equation was evaluated by analysis of variance (ANOVA) (Table 4). The significance of each coefficient was assessed using the p-value; the coefficient will be more significant, the lower its p-value. The significance of model equation was statistically evaluated by calculating the p-value with the significance level of 95% ($p < 0.05$). The p-value for lack of fit was used to check the adequacy of the model equation. The coefficient of determination (R^2) and the adjusted coefficient of determination (R^2_{Adj}) were used to evaluate the goodness of fit of the model, besides the pure error was determined to know the good reproducibility of the experimental data [39]. Moreover, the mean square error (MSR) is shown in Table 3.

The p-value of the lack of fit was 0.07498 ($p > 0.05$), demonstrating that was statistically insignificant, which confirmed the goodness-of-fit and suitability of regression model [32,40]. Consequently, the model was suitable for describing the relationship between the variables and the response. This can be appreciated in Fig. 6 by comparing the experimental values (actual) in x-axis against the predicted responses in y-axis, due to the data points are closed to the fitted line.

The determination coefficient (R^2= 0.99385) reveals that the model, thus adjusted, explains 99.385% of the variability in FAME, only 0.61% of the total variation was not explained by the model. The adjusted determination coefficient (R^2_{Adj}= 0.98278) further attested to the minimal difference between the experimental and predicted values. According to Hashemzadeh and Sadrameli [22], for the model to be able to significantly predict the response and explain 95% of the variability, the difference of these two coefficients (R^2 and R^2_{Adj}) must be less than 0.2. This condition is fulfilled in this case. Moreover, the high value of the R^2_{Adj} implied the significance of the model parameters. The good reproducibility of the experimental data is reflected by the low value of pure error of this model.

Table 4 demonstrated that the linear coefficients (X_1, X_2, X_3), the X_2^2 and X_3^2 quadratic term coefficients, and the $X_1 \times_2$ and $X_1 \times_3$ cross-product coefficients were significant model terms ($p < 0.05$), while the X_1^2 quadratic term coefficient and the $X_2 \times_3$ cross-product coefficient were insignificant to the response ($p > 0.05$).

In addition, Fig. 7 shows the Pareto chart, which allows discussing the individual effects of the variables as well as their interactions and the quadratic effects. The length of the horizontal blocks is proportional to the absolute value of its associated regression coefficient or estimated effect. The order in which the blocks are presented agrees to the order of the size of the effect. Moreover, the vertical line indicates the statistical significance (corresponds to the 95% limit); then an effect is significant if its horizontal block crosses the line [41].

As it was shown in Fig. 7, MeOH/oil molar ratio (X_2) has the largest influence on the FAME content. In contrast, the cross effect of the MeOH/oil molar ratio and the DEE/MeOH molar ratio, and the quadratic effect of flow rate were not significant. These results agree with those of Table 4.

Table 3
Box-Behnken experimental design matrix and the response of dependent variable.

Run	Independent variables Flow rate ± 0.05(mL min^{-1})	MeOH/oil molar ratio ± 0.01	DEE/MeOH molar ratio ± 0.5	FAME (%) Experimental* ± 0.1	Predicted	Residual	MSE
1	1.4	6	1	52.6	53.4	−0.8	0.64
2	1.4	20	1	97.6	98.5	−0.9	0.81
3	0.7	20	1	98.7	97.9	0.8	0.64
4	1.4	13	0.5	87.3	85.1	2.2	4.84
5	0.7	13	0.5	85.2	84.6	0.6	0.36
6	1.4	13	1.5	71.8	72.5	−0.7	0.49
7	0.7	6	1	63.2	62.3	0.9	0.81
8	1.05	20	0.5	96.9	98.3	−1.4	1.96
9	0.7	13	1.5	79.0	81.2	−2.2	4.84
10	1.05	20	1.5	92.4	91.0	1.4	1.96
11	1.05	6	0.5	57.2	58.7	−1.5	2.25
12	1.05	6	1.5	51.3	49.9	1.4	1.96
13	1.05	13	1	83.6	84.3	−0.7	0.49
14	1.05	13	1	85.1	84.3	0.8	0.64
15	1.05	13	1	84.2	84.3	−0.1	0.01
							1.51

*Average of three replications.

Table 4
Analysis of variance (ANOVA) for the regression model equation.

Sources of variation	Sum of squares	Degrees of freedom	Mean square	F-value	P-value	Comment
X_1	35.28	1	35.28	61.89	0.0158	Significant
X_2	3252.21	1	3252.21	5705.63	0.0002	Significant
X_3	128.80	1	128.80	225.97	0.0044	Significant
X_1^2	9.23×10^{-3}	1	9.23×10^{-3}	0.02	0.9104	Not significant
$X_1\times_2$	22.56	1	22.56	39.58	0.0243	Significant
$X_1\times_3$	21.62	1	21.62	37.93	0.0254	Significant
X_2^2	147.71	1	147.71	259.15	0.0038	Significant
$X_2\times_3$	0.49	1	0.49	0.86	0.4517	Not significant
X_3^2	45.88	1	45.88	80.49	0.0122	Significant
Lack of fit	21.42	3	7.14	12.52	0.0748	Not significant
Pure error	1.14	2	0.57			
Total	3667.65	14				

R^2= 0.99385, R^2_{Adj}= 0.98278.

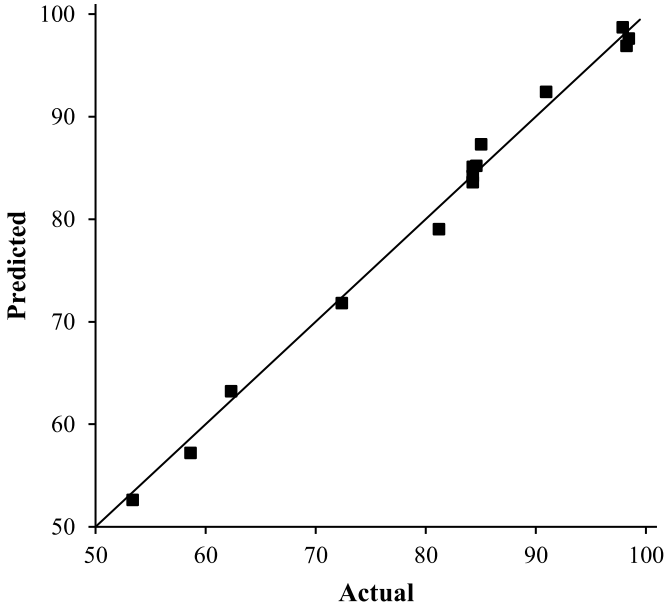

Fig. 6. Predicted versus actual%FAME content.

3.3. Main effect of variables on the FAME content

The main effects plot (Fig. 8) illustrates the effect of changing each factor while keeping all the others at a constant level. The sensitivity of the response to that factor is determined by a steep slope or curvature [42]. The curvature shown by the MeOH/oil molar ratio indicates that it is the most influential factor on the FAME content, followed by the DEE/MeOH molar ratio. The flow rate shows the flattest curve, demonstrating that is the least significant parameter of the three on the FAME content.

3.3.1. Effect of flow rate

Flow rate and residence time are inversely correlated. In continuous biodiesel production, residence time is one of the most important variables that can affect the activity of the catalytic packed-bed and, then, to the FAME yield. Therefore, the impact of flow rate on FAME content was studied at range of 0.7 to 1.4 min^{-1}. As shown in Fig. 8, a decrease in flow rate results in a high FAME content. This is because the lower the flow rate, the longer the residence time, which means a longer contact time between the reactants and the catalyst in the column, allowing to convert the triglycerides of the oil into methyl esters of biodiesel. For high flow rates the conversion of triglycerides to esters is lower since a lower FAME content is obtained.

3.3.2. Effect of MeOH/oil molar ratio

In the transesterification reaction for biodiesel production, the stoichiometric molar ratio of methanol to triglyceride is 3:1 [43,44]. However, in practice a higher MeOH/oil molar ratio is necessary for the reaction to proceed completely and therefore methanol could increase production costs. For this reason, it is necessary to know the optimal methanol/oil molar ratio. To investigate the effect of the MeOH/oil molar ratio, this parameter was varied in the range 6:1–20:1. In the main effects plot (Fig. 8) it can be seen that the MeOH/oil molar ratio factor

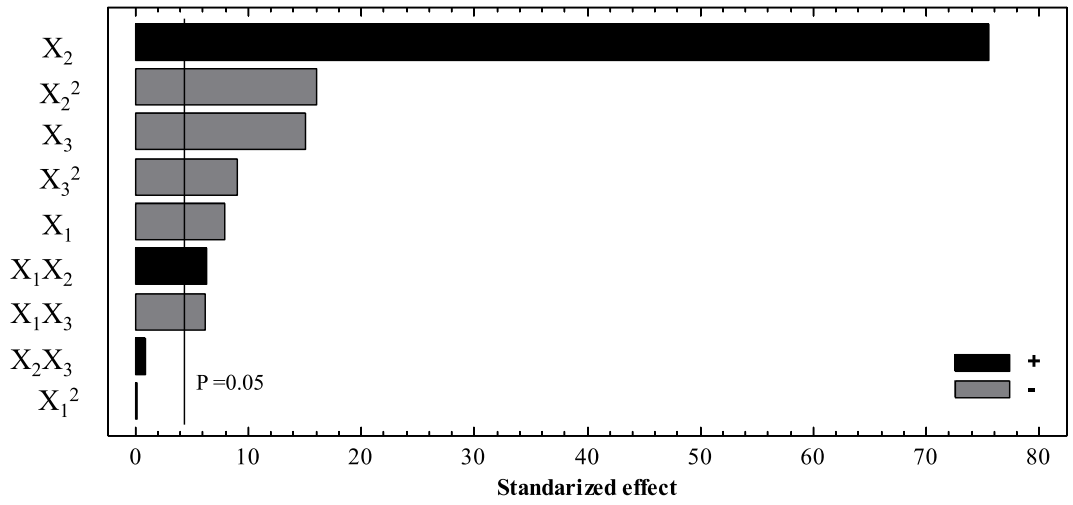

Fig. 7. Pareto chart of standardized effects for FAME content.

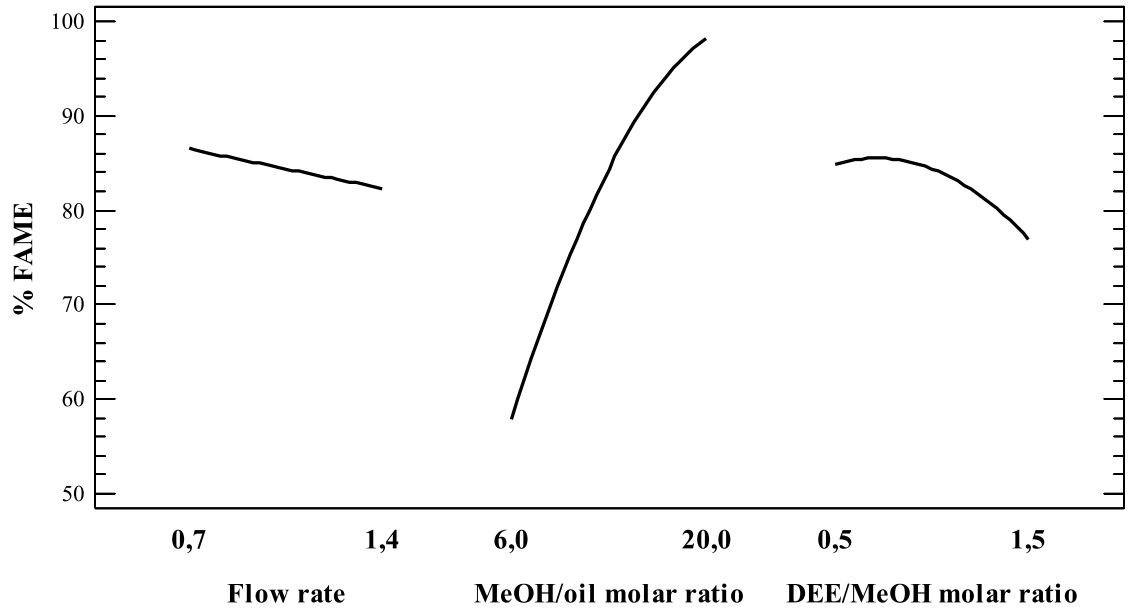

Fig. 8. Main effects plot for FAME content.

has a significant impact on the FAME content of the biofuel obtained, since when the MeOH/oil molar ratio is increased, the FAME content increases considerably.

3.3.3. *Effect of DEE/MeOH molar ratio*

The cosolvent/alcohol molar ratio is one essential factor that directly affect the FAME yield. Mass transfer between the phases (alcohol and oil) and the solid catalyst considerably decreases the reaction rate. The addition of a cosolvent can solve this issue; however, high amounts of cosolvent could adversely affect the FAME yield [34]. In this work, the influence of DEE/MeOH molar ratio on the FAME yield was analyzed at range of 0.5:1–1.5:1. The use of DEE as cosolvent improves the mass transfer between the phases and high FAME yield are achieved even at low temperature (40 °C). Fig. 8 show that, at low DEE/MeOH molar ratio, the FAME content enhanced by increasing the DEE/methanol molar ratio; however, at high DEE/MeOH molar ratio, a decrease in the FAME content was observed, this is because the excess of DEE could favor the presence of FAME and glycerol in the same phase, giving rise to the reduction of the reaction rate and the FAME yield [45]. Economically, the need for low amounts of cosolvent is an advantage; in addition, DEE creates a homogeneous solution from oil and methanol and therefore, this can appropriately be in contact with the catalyst particles that were packed in the reactor [29].

3.4. *Interaction effect of variables on the FAME content*

The obtained regression model was used to calculate the response surface. Estimated response surface profiles and its related contours are shown in Figs. 9-11. Figs. 9a-11a show the response surface plots for FAME content as a function of flow rate and MeOH/oil molar ratio (Fig. 9a), MeOH/oil molar ratio and DEE/MeOH molar ratio (Fig. 11a) and flow rate and DEE/MeOH molar ratio (Fig. 10a); in all cases, the third variable was set at a constant value.

In Fig. 9 the interaction effect on FAME content of flow rate and MeOH/oil molar ratio at constant DEE/MeOH molar ratio (1:1) is presented. It was observed that at low flow rate and MeOH/oil molar ratio, low FAME content was attained (66.39% at 0.7 mL min^{-1} and a MeOH/oil molar ratio of 7:1). At the same MeOH/oil molar ratio (7:1) and 1.4 mL min^{-1}, the FAME content decreased slightly (58.12%). However, FAME content increases considerably with the rise in MeOH/oil molar

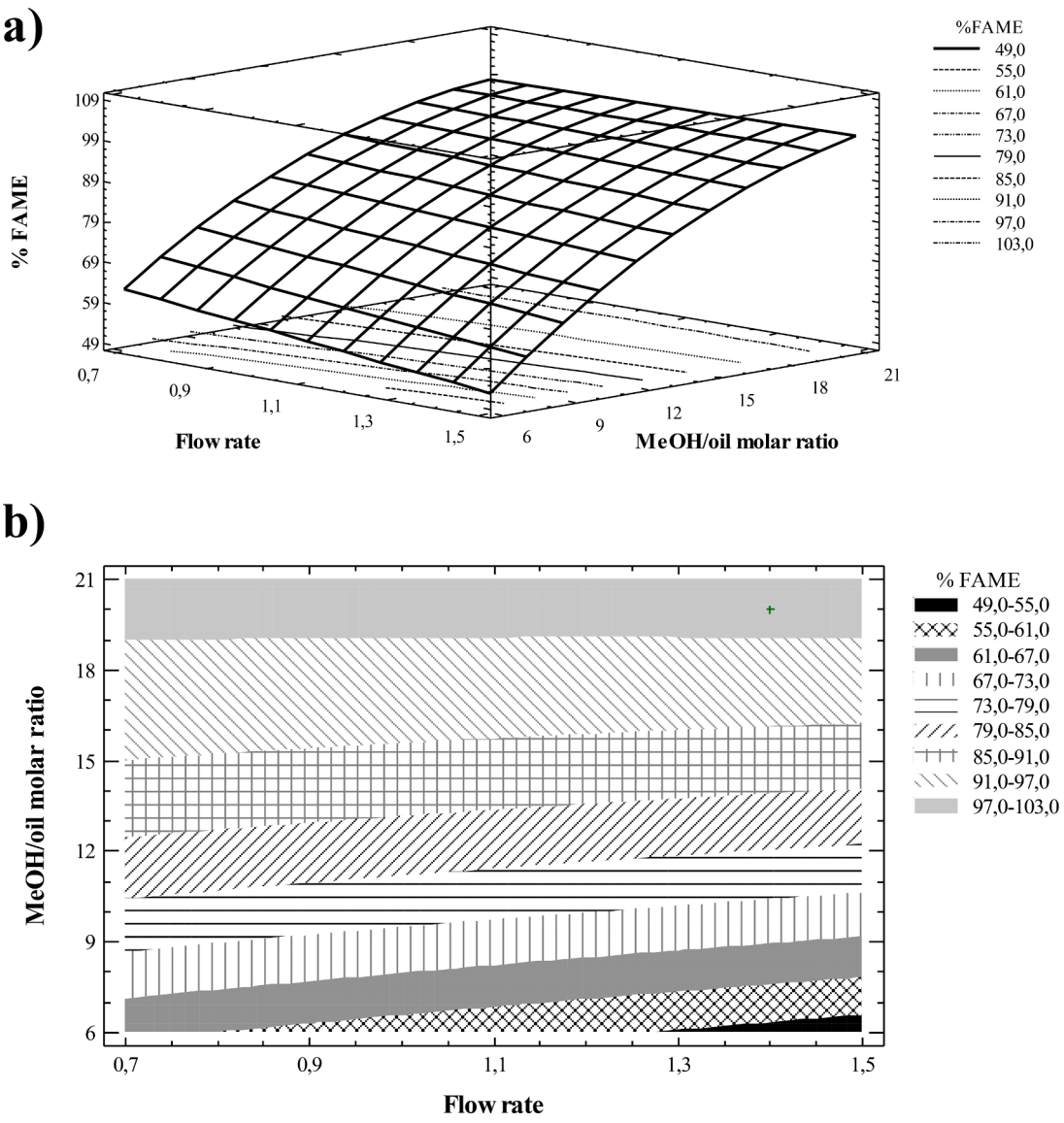

Fig. 9. (a) 3D response surface profile and (b) contour plot for the interaction between flow rate and MeOH/oil molar ratio on FAME content (DEE/MeOH molar ratio=1.0).

ratio, being the variable that most influences this model. A maximum FAME content (97.0–103.0%) was obtained for MeOH/oil molar ratios greater than 18:1 and regardless of the flow rate (Fig. 9a). Transesterification is a reversible reaction, so an excess of methanol is required to shift the reaction in the direction of the products [46]. A low flow rate and a high MeOH/oil molar ratio seem more suitable to reach the maximum yield. Maximum FAME content (97.75%) was achieved at 1.4 mL min^{-1} flow rate and 20:1 MeOH/oil molar ratio (Fig. 9b).

The interaction of the MeOH/oil molar ratio and DEE/MeOH molar ratio on the FAME content at a 1.05 mL min^{-1} flow rate is shown in Fig. 10. As shown in contour plot (Fig. 10b), at a low MeOH/oil molar ratio of 8:1 and low DEE/MeOH molar ratio of 0.5:1, a FAME content of 67.21% was obtained; whereas at the same DEE/MeOH molar ratio but for MeOH/oil molar ratios greater than 19:1, the maximum FAME contents were achieved (97.0–103.0%). For high values of the MeOH/oil molar ratio and values of the DEE/MeOH molar ratio lower than 1.2:1, high FAME contents were also obtained. However, an increase in the DEE/MeOH molar ratio involves a decrease in the FAME content. Maximum FAME content (98.09%) was achieved at 20:1 MeOH/oil molar ratio and around about 0.6:1 DEE/MeOH molar ratio and (Fig 10b).

The effect of flow rate and DEE/MeOH molar ratio at the constant MeOH/oil molar ratio of 13:1 is presented in Fig. 11. The highest FAME contents (85.0–91.0%) were obtained at high flow rates and a low DEE/MeOH molar ratio or, if low flow rates are used, with low DEE/MeOH molar ratios, but in a broader range as shown in the contour plot (Fig. 11b). Maximum yield of biodiesel (85.0%) was achieved at 1.4 mL min^{-1} flow rate and 0.6:1 DEE/MeOH molar ratio.

In general, FAME contents of more than 96.5%, according to EN 14,214 standard, could be achieved with a high MeOH/oil molar ratio and low values of the flow rate and DEE/MeOH molar ratio.

3.5. *Optimization process*

Optimization was performed through statistical analysis using BBD to attain the maximum FAME yield based on the fitted model (Eq. (3)). The optimization criteria and the optimum conditions for continuous biodiesel production from *Jatropha curcas* oil using Li/Pumice as solid catalyst in a packed-bed reactor assisted with DEE as cosolvent are given in Table 5. The process optimization model suggested the optimal values of the different independent variables of the process as 1.4 mL min^{-1} flow rate, 20:1 MeOH/oil molar ratio and 0.57:1 DEE/MeOH molar ratio

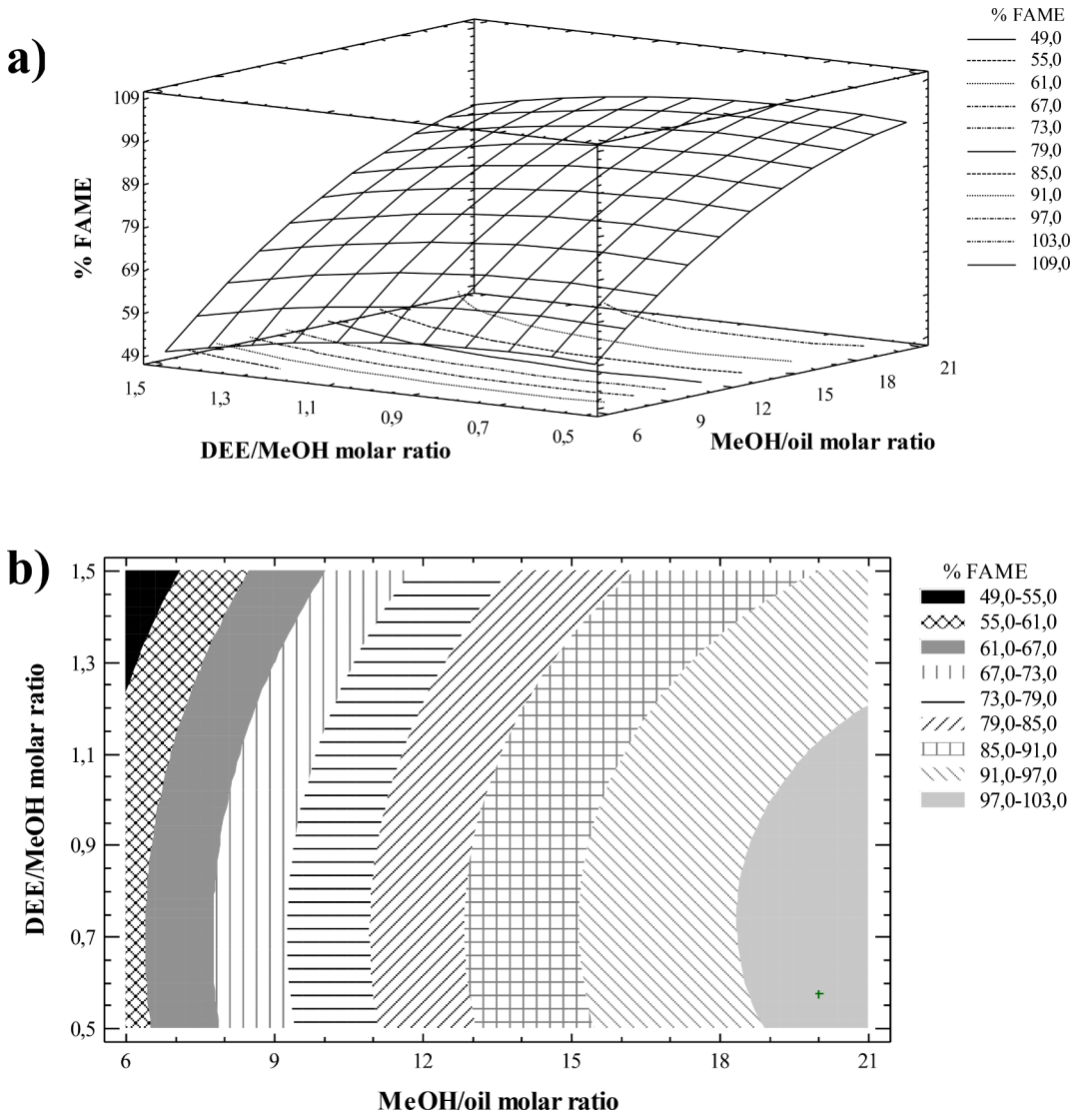

Fig. 10. (a) 3D response surface profile and (b) contour plot for the interaction between MeOH/oil molar ratio and DEE/MeOH molar ratio on FAME content (flow rate=1.05 mL min^{-1}).

to achieve the maximum FAME yield (100%). Once the optimum conditions were obtained, three experiments were carried out under those conditions and it was observed that the corresponding experimental values of FAME yield were found to be 100%, which were close to the optimized value.

Some authors found similar results when they evaluated the effect of several parameters of reaction on the purity of the biodiesel through the response surface methodology. Gouran et al. [5] investigated the transesterification of waste cooking oil using modified wheat bran ash and CaO as the catalyst. A biodiesel purity of 93.6% was obtained under the following optimal condition: methanol to oil volume ratio of 1.46:1, a catalyst content of 11.66 wt%, and a temperature of 54.6 °C during 114.21 min). Aghel et al. [6] studied the transesterification of waste cooking oil as feedstock and clinoptilolite/CaO as a catalyst. Under optimized conditions (the oil to methanol volume ratio of 1.47, the catalyst dosage of 8.08 wt%, the temperature of 54.72 °C, and the duration of 119 min) the highest purity of biodiesel for waste cooking oil was 84.76%. Mohadesi et al. [7] investigated the use of clay/CaO heterogeneous catalyst to produce biodiesel from waste cooking oil. Under optimal conditions (temperature of 54.97 °C, catalyst concentration of 9.6 wt%, oil to methanol volume ratio of 1.94 v/v, toluene concentration of 16.13 wt%, and reaction time of 74.32 min) the conversion rate was 97.16%.

The use of a small amount of DEE as cosolvent enhances the mass transfer between the phases present in the packed-bed transesterification process and high FAME yield is achieved even at low temperature (40 °C). Those are results very encouraging when compare with the high temperature needed when no cosolvent is used. Therefore, the addition of DEE is beneficial for the saving of energy and operating cost. Furthermore, the Li/Pumice catalyst proved to be a promising heterogeneous catalyst for the continuous biodiesel production at low temperature.

3.6. Stability of the catalyst

The reusability is one of the most significant characteristics of a solid catalyst. The ability to reuse the Li/Pumice catalyst in the transesterification of *Jatropha curcas* oil was investigated for 8 h reaction under the optimal conditions and the results are shown in Fig. 12. The solid catalyst was used directly for 8 h without any type of treatment.

It was observed that at short reaction times (less than 90 min) the stability of the system has not been achieved, since%FAME obtained were slightly lower than those obtained under the optimal conditions. At 90 min a 100% FAME was reached, and this remains practically constant

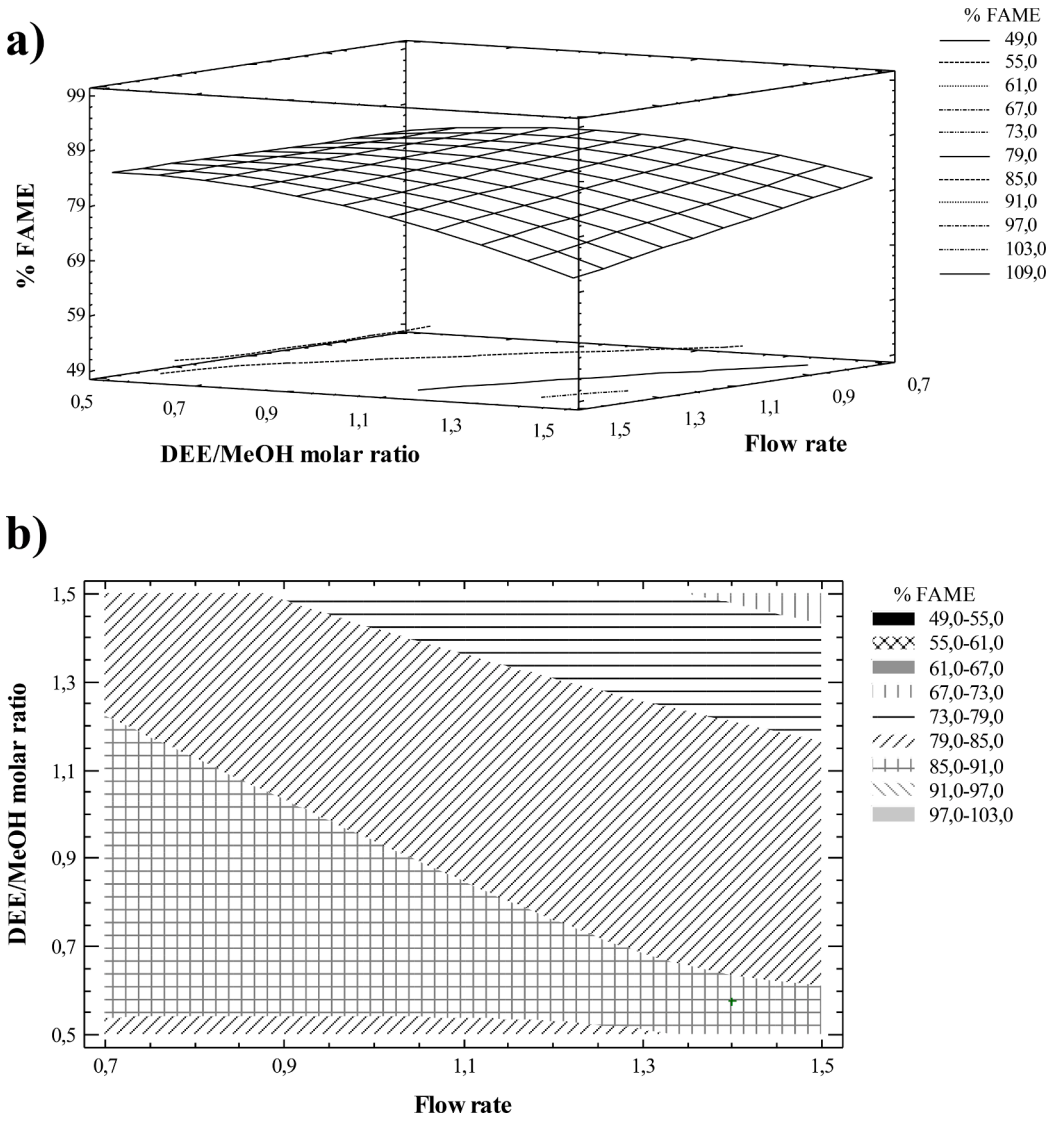

Fig. 11. (a) 3D response surface profile and (b) contour plot for the interaction between flow rate and DEE/MeOH molar ratio on FAME content (MeOH/oil molar ratio=13.0).

Table 5
Optimization criteria for maximum FAME yield and optimum conditions.

		Lower limit	Upper limit	Optimum
Independent variables (factors)	Flow rate (mL min^{-1})	0.7	1.4	1.4
	MeOH/oil molar ratio	6.0	20.0	20.0
	DEE/MeOH molar ratio	0.5	1.5	0.57
Dependent variable	FAME (%)	Maximize		100%

for 8 h, with percentages higher than the minimum established by regulations (96.5%). These results show the high stability of the heterogeneous Li/Pumice catalyst for the continuous biodiesel production when compared to other heterogeneous catalysts found in the literature. Borah et al. [47] and Goli and Sahu [48] studied the reusability of Zn/CaO catalyst and eggshell waste derived CaO catalyst, respectively. In both studies, a high FAME yield was achieved in the first cycle, but a gradual drop-in catalytic activity was observed after each run. According to the authors, the cause of the decrease in the activity of the catalysts is due to the leaching of the active site to the alcoholic phase or the

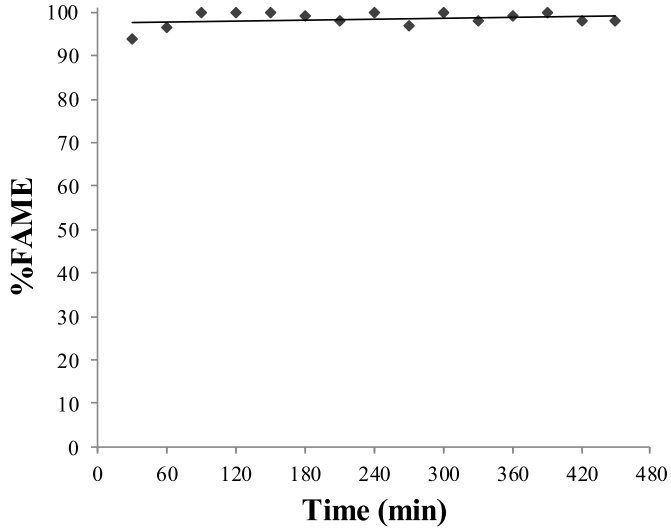

Fig. 12. Stability of the Li/Pumice catalyst.

blockage of catalysts active sites by products formed during the transesterification reaction [47,48].

In this work, the synthesis method appears to be appropriate since it appears that there is no leaching during the test time. However, for future research, longer production times can be investigated, analyzing how they affect the catalyst activity. Furthermore, a physical and chemical characterization of the catalyst used during long reaction times can be carried out to understand its behavior.

4. Conclusions

In this work, a packed-bed reactor using Li/Pumice as a solid catalyst was developed for biodiesel production in continuous. The continuos transesterification of *Jatropha curcas* oil assisted with DEE as a cosolvent allowed to produce biodiesel at low temperature (40 °C). RSM based on three variable BBD was employed to establish the relationship between the factors and the FAME content. The influence of the three factors (flow rate (0.7–1.4 mL/min), MeOH/oil molar ratio (6:1–20:1) and DEE/MeOH molar ratio (0.5:1–1.5:1)) on the FAME content was investigated. The values of the response variable predicted by the model are in good agreement with the values determined experimentally (R^2= 0.99385, R^2_{Adj}= 0.98278). The optimal reaction conditions for the continuous biodiesel production were evaluated (1.4 mL min^{-1} flow rate, 20:1 MeOH/oil molar ratio and 0.57:1 DEE/MeOH molar ratio). Under these optimum conditions, the maximum FAME content was 100%, complying with the standards established by regulations (≥96.5%FAME). In addition, Li/Pumice showed high stability since no decrease in activity was observed over long reaction times. Li/Pumice and DEE, used as catalyst and cosolvent, respectively, is a suitable system for obtaining biodiesel continuously from renewable feedstock such as *Jatropha curcas*.

Declaration of Competing Interest

The authors declare that they have no known competing financial interests or personal relationships that could have appeared to influence the work reported in this paper.

Data Availability

The datasets used and/or analyzed during the current study are available from the corresponding author on reasonable request.

Acknowledgments

This research has been co-funded by FEDER funds. INTERREG MAC 2014–2020 program within the ACLIEMAC project (MAC2/3.5b/380) and by "Fundación CajaCanarias" and "Fundación Bancaria "la Caixa"" through the "Convocatoria Proyectos Investigación 2019″. Authors would like also to acknowledge to the General Service Research Support of the Universidad de La Laguna for their instrumental and technical support.

Statement of novelty and significance

The use of heterogeneous catalysts for continuous biodiesel production is advantageous. Currently, on the industrial scale biodiesel production, slurry batch reactors are employed to carry out the transesterification reaction due to homogeneous catalysts are used. Batch processes are characterized by low productiveness and high operating costs. The use of a packed-bed catalytic reactor system shows clearly advantages compared with a slurry batch reactor system from a products separation and simple operation point of view. Furthermore, the use of a cosolvent allows overcoming the mass transfer limitations that exist due to the immiscibility of the oil and alcohol.

Author contribution

Díaz, L: conceptualization, methodology, data analysis, writing, and reviewing and editing.

Escalante, D.: conceptualization, material preparation, data analysis and writing.

Rodríguez, K.E.: conceptualization, supervision, data analysis and validation.

Kuzmina, Y.: material preparation, data collection and analysis.

González, L.A.: conceptualization, funding acquisition, project administration and reviewing.

References

[1] H.F. Gerçel, A.E. Pütün, E. Pütün, Hydropyrolysis of extracted Euphorbia rigida in a well-swept fixed-bed tubular reactor, Energy Sources 24 (2002) 423–430.
[2] R. Ma, M.A. Hanna, Biodiesel production: a review, Bioresour. Technol. 70 (1999) 1–15.
[3] D. Kusdiana, S. Saka, Kinetics of transesterifcation in rapeseed oil to biodiesel fuel as treated in supercritical methanol, Fuel 80 (2001) 693–698.
[4] D. Kusdiana, S. Saka, Methyl esterification of free fatty acids of rapeseed oil as treated in supercritical methanol, J. Chem. Eng. Jpn. 34 (2001) 383–387.
[5] A.n Gouran, B. Aghel, F. Nasirmanesh, Biodiesel production from waste cooking oil using wheat bran ash as a sustainable biomass, Fuel 295 (2021), 120542.
[6] B. Aghel, A. Gouran, F. Nasirmanes, Transesterification of waste cooking oil using clinoptilolite/industrial phosphoric waste as green and environmental catalysts, Energy 244 (2022), 123138. Part B.
[7] M. Mohadesi, B. Aghel, A. Gouran, M. Hamed Razmehgir, Transesterification of waste cooking oil using Clay/CaO as a solid base catalyst, Energy 242 (2022), 122536.
[8] D.-.T. Tran, J.-.S. Chang, D-J. Lee, Recent insights into continuous-flow biodiesel production via catalytic and non-catalytic transesterification processes, Appl. Energy 185 (2017) 376–409.
[9] C.V. McNeff, L.C. McNeff, B. Yan, D.T. Nowlan, M. Rasmussen, A.E. Gyberg, B. J. Krohn, R.L. Fedie, A continuous catalytic system for biodiesel production, Appl. Catal. A 343 (2008) 39–48.
[10] M.E. Borges, J.C. Ruiz-Morales, L. Díaz, Improvement of biodiesel production through microstructural engineering of a heterogeneous catalyst, J. Ind. Eng. Chem. 19 (3) (2013) 791.
[11] F. Galli, L. Bonfanti, S. Capelli, F. Manenti, C.L. Bianchi, G.S. Patience, C. Pirola, Heterogeneous oil transesterification in a single-phase liquid mixture using a cosolvent for improved biofuels production, Energy Technol. 3 (12) (2015) 1170–1173.
[12] J.M. Encinar, A. Pardal, N. Sánchez, An improvement to the transesterification process by the use of cosolvents to produce biodiesel, Fuel 166 (2016) 51–58.
[13] Z.B. Todorović, D.Z. Troter, D.R. Đokić-Stojanović, A.V. Veličković, J. M. Avramović, O.S. Stamenković, L.M. Veselinović, V.B. Veljković, Optimization of CaO-catalyzed sunflower oil methanolysis with crude biodiesel as a cosolvent, Fuel 237 (2019) 903–910.
[14] P. Soares Dias, M. Ramos, M. Catarino, J. Puna, J. Gomes, Solvent assisted biodiesel production by co-processing beef tallow and soybean oil over calcium catalysts, Waste Biomass Valoris. 11 (2020) 6249–6259, volume.
[15] Y. Alhassan, N. Kumar, I.M. Bugaje, H.S. Pali, P. Kathkar, Cosolvents transesterification of cotton seed oil into biodiesel: effects of reaction conditions on quality of fatty acids methyl esters, Energy Convers. Manag. 84 (2014) 640–648.
[16] C.M.F. Casas, M.J. Ramos, A. Pérez, J.F. Rodríguez, Optimization of the reaction parameters for fast pseudo single-phase transesterification of sunflower oil, Fuel 89 (3) (2010) 650–658.
[17] S. Sakthivel, S. Halder, P. Gupta, Influence of cosolvent on the production of biodiesel in batch and continuous process, Int. J. Green Energy 10 (8) (2013) 876–884.
[18] R. Pena, R. Romero, S.L. Martínez, M.J. Ramos, A. Martínez, A. Martínez, Transesterification of castor oil: effect of catalyst and cosolvent, Ind. Eng. Chem. Res. 48 (2009) 1186–1189.
[19] G. Guan, K. Kusakabe, N. Sakurai, K. Moriyama, Transesterification of vegetable oil to biodiesel fuel using acid catalysts in the presence of dimethyl ether, Fuel 88 (2009) 81–86.
[20] U.N. Soriano, R. Venditti, S.D. Argyropoulos, Biodiesel synthesis via homogenous Lewis-acid-catalyzed transesterification, Fuel 88 (2009) 560–565.
[21] I.A. Mohammed-Dabo, M.S. Ahmad, A. Hamza, K. Muazu, A. Aliyu, Cosolvent transesterification of Jatropha curcas seed oil, J. Pet. Technol. Altern. Fuels 3 (4) (2012) 42–51.
[22] M. Hashemzadeh Gargari, S.M. Sadrameli, Investigating continuous biodiesel production from linseed oil in the presence of a Cosolvent and a heterogeneous based catalyst in a packed bed reactor, Energy 148 (2018) 888–895.
[23] H. Zhang, Y.L. Li, X.G. Wu, Y.J. Zhang, D.B Zhang, Application of response surface methodology to the treatment landfill leachate in a three-dimensional electrochemical reactor, Waste Manag. 30 (2010) 2096–2102.
[24] D.Vujević Grčić, J. Šepčić, N. Koprivanac, Minimization of organic content in simulated industrial wastewater by Fenton type processes: a case study, J. Hazard. Mater. 170 (2009) 954–961.

[25] H.Zhang Wu, N. Oturan, Y. Wang, L. Chen, M.A. Oturan, Application of response surface methodology to the removal of the antibiotic tetracycline by electrochemical process using carbon-felt cathode and DSA (Ti/RuO2–IrO2) anode, Chemosphere 87 (2012) 614–620.
[26] P.C. Nnaji, V.C. Anadebe, O.D. Onukwuli, et al., Multifactor optimization for treatment of textile wastewater using complex salt–Luffa cylindrica seed extract (CS-LCSE) as coagulant: response surface methodology (RSM) and artificial intelligence algorithm (ANN–ANFIS), Chem. Pap. 76 (2022) 2125–2144.
[27] T.M.I. Riayatsyah, A.H. Sebayang, A.S. Silitonga, Y. Padli, I.M.R. Fattah, F. Kusumo, H.C. Ong, T.M.I. Mahlia, Current progress of jatropha curcas commoditisation as biodiesel feedstock: a comprehensive review, Front. Energy Res. 9 (2022), 815416.
[28] A. Torres, B. Fuentes, K.E. Rodríguez, A. Brito, L. Díaz, Analysis of the content of fatty acid methyl esters in biodiesel by fourier-transform infrared spectroscopy: method and comparison with gas chromatography, J. Am. Oil Chem. Soc. 97 (2020) 651–661.
[29] N. Shibasaki-Kitakawa, H. Honda, H. Kuribayashi, T. Toda, T. Fukumura, T. Yonemoto, Biodiesel production using anionic ion-exchange resin as heterogeneous catalyst, Bioresour. Technol. 98 (2007) 416–421.
[30] N.H. Zabaruddin, N.H. Mohamed, L.C. Abdullah, M. Tamada, Y. Ueki, N. Seko, T.S. Y. Choong, Palm oil-based biodiesel synthesis by radiation-induced kenaf catalyst packed in a continuous flow system, Ind. Crops Prod. 136 (2019) 102–109.
[31] UNE, UNE-EN 14103:2020: Fat and Oil Derivatives—Fatty Acid Methyl Esters (FAME)—Determination of Ester and Linolenic Acid Methyl Ester Contents, Asociacion Espanola de Normalizacion y Certificacion (AENOR), 2020.
[32] N. Chueluecha, A. Kaewchada, At. Jaree, Enhancement of biodiesel synthesis using cosolvent in a packed-microchannel, J. Ind. Eng. Chem. 51 (2017) 162–171.
[33] S.L.C. Ferreira, R.E. Bruns, H.S. Ferreira, G.D. Matos, J.M. David, G.C. Brandao, E. G.P.D. Silva, L.A. Portugal, P.S.D. Reis, A.S. Souza, W.N.L.D. Santos, Box-Behnken design: an alternative for the optimization of analytical methods, Anal. Chim. Acta 597 (2007) 179.
[34] K.Huang Wu, T. Wei, Z. Lin, Y. Zou, Z. Tong, Process intensification of NaOH-catalyzed transesterification for biodiesel production by the use of bentonite and co-solvent (diethyl ether), Fuel 186 (2016) 597–604.
[35] I. Lukic, J. Krstic, S. Glisic, D. Jovanovic, D. Skala, Biodiesel synthesis using K2CO3/Al-O-Si aerogel catalysts, J. Serb. Chem. Soc. 75 (2010) 789–801.
[36] J. Temuujin, K. Okada, K.J.D. MacKenzie, Preparation and properties of potassium aluminosilicate prepared from the waste solution of selectively leached calcined kaolinite, Appl. Clay Sci. 21 (2002) 125–131.
[37] G. Neri, G. Rizzo, L. De Luca, F. Corigliano, I. Arrigo, A. Donato, Zeolitized-pumice as a new support for hydrogenation catalysts, Catal. Commun. 9 (2008) 2085–2089.
[38] N. Inchaurrondo, A. Maestre, G. Zerjav, A. Pintar, C. Ramos, P. Haure, Screening of catalytic activity of natural iron-bearing materials towards the catalytic wet peroxide oxidation of orange II, J. Environ. Chem. Eng. 6 (2) (2018) 2027–2040.
[39] E.D. Rodríguez Martínez, Eficiencia de Activadores Alcalinos Basados En Diferentes Fuentes De Sílice Para La Producción De Sistemas Geopoliméricos De Cenizas Volante. Trabajo De Investigación CST/MIH-05, Universidad Politécnica de Valencia. Valencia, 2009.
[40] Y. Liu, F. Liu, L. Ni, M. Meng, Xi. Meng, G. Zhongb, J. Qiua, A modeling study by response surface methodology (RSM) on Sr(II) ion dynamic adsorption optimization using a novel magnetic ion imprinted polymer, RSC Adv. 6 (2016) 54679–54692.
[41] T. Fan, J. Hu, L. Fu, L. Zhang, Optimization of enzymolysis-ultrasonic assisted extraction of polysaccharides from Momordica charabtia L. by response surface methodology, Carbohydr. Polym. 115 (2015) 701–706.
[42] S.A. Rezzoug, C. Boutekedjire, K. Allaf, Optimization of operating conditions of rosemary essential oil extraction by a fast controlled pressure drop process using response surface methodology, J. Food Eng. 71 (2005) 9–17.
[43] M. Kirubakaran, V.A.M. Selvan, Eggshell as heterogeneous catalyst for synthesis of biodiesel from high free fatty acid chicken fat and its working characteristics on a CI engine, J. Environ. Chem. Eng. 6 (2018) 4490–4503.
[44] W.L. Xie, H. Peng, L.G. Chen, Calcined Mg-Al hydrotalcites as solid base catalyst for methanolysis of soybean oil, J. Mol. Catal. A Chem. 246 (2006) 24–32.
[45] E. Borges, L. Díaz, Catalytic packed-bed reactor configuration for biodiesel production using waste oil as feedstock, Bioenergy Res. 6 (2013) 222–228.
[46] L.T. Thanh, K. Okitsu, Y. Sadanaga, N. Takenaka, Y. Maeda, A new co-solvent method for the green production of biodiesel fuel—optimization and practical application, Fuel 103 (2013) 742–748.
[47] J. Borah, A. Dasa, V. Dasa, N. Bhuyanb, D. Dekaa, Transesterification of waste cooking oil for biodiesel production catalysed by Zn substituted waste egg shell derived CaO nanocatalyst, Fuel 242 (2019) 345–354.
[48] J. Goli, O. Sahu, Development of heterogeneous alkali catalyst from waste chicken eggshell for biodiesel production, Renew. Energy 128 (2018) 142–154.